

# Oxygen mass transfer in liquids

Emmanouil Papadakis, Kevin Klejn and Per Stobbe<sup>1</sup>

*CerCell ApS*, Malmlosevej 19C, DK-2840 Holte, Denmark

## Abstract

In this project, oxygen mass transfer in liquids through the use of different bubble generation equipment is examined. The purpose of this project, is to first investigate the bubble formation through different type of spargers made from different materials and different governing oxygen transfer phenomena. Based on the analysis of the investigations, equipment weaknesses that might be crucial for some applications are identified and finally, an equipment design, which eliminates the identified weaknesses, is proposed and validated.

The findings of this investigation are to be used to replace a steel sparger attached on L-shaped tube with a single-use sparger (made of plastic) attached on a straight tube that generates the same or better bubbles in terms of shape, size and size distribution. A metal sparger attached on L-shaped tube, a cylindrical plastic sparger attached on L-shaped tube and porous disks on different sparger bodies attached on L-shaped tube were initially tested and compared. Moreover, tests of the cylindrical plastic sparger (called “Frit”) attached on a straight tube and L-shaped tubes with 2 and 3 orifices, which are commonly used, were performed. Through the analysis, it has been concluded that bubbles formed through porous material, especially for the single use plastic sparger, are better in terms of bubble size distribution, bubble size, and application range. Additionally, it has been observed that larger bubbles and/or bubbles with irregular shapes are formed through the joint points and through flat surfaces of the sparger facing towards the bottom of the reactor, these bubbles also appear to have higher possibilities to be involved in coalescing phenomena close to the sparger’s surface.

Finally, two improved designs have been proposed where all the joint points are sealed, the mass transfer resistance has been increased on the surface facing towards the bottom of the reactor with the only difference that in one design the flat surfaces have been eliminated and in the other the flat surfaces have remained.



---

<sup>1</sup> Contact information: Per Stobbe [per.stobbe@cercell.com](mailto:per.stobbe@cercell.com), Kevin Klejn [kevin.klejn@cercell.com](mailto:kevin.klejn@cercell.com), Emmanouil Papadakis, [em.papadakis@outlook.com](mailto:em.papadakis@outlook.com)

# Contents

Abstract .....	1
1 Short introduction .....	7
2 Materials and methods .....	9
2.1 Airflow calibration .....	11
2.2 Method.....	11
3 Results.....	11
3.1 Step1. Problem definition.....	12
3.2 Step 2. Testing.....	12
3.3 Step 3. Evaluation and identification .....	12
3.3.1 Test 1. Evaluate the bubble size distribution in bioreactors using different sparger types attached on L-shaped tube. ....	12
3.3.2 Test 2. Evaluate bubble generation and coalescing phenomena.....	20
3.3.3 Test 3. Comparison of a straight tube with cylindrical plastic sparger with an L-shaped tube with metallic sparger. ....	21
3.3.4 Test 4. Bubble generxation through non-porous material with 2 and 3 orifices (SIZE of orifices).....	23
3.3.5 Observations and discussion on bubble generation .....	25
3.3.6 Possible solutions:.....	25
3.4 Step. 4. Suggestions and testing .....	26
3.5 Step 5. Final Validation.....	29
4 Discussion and Conclusion .....	30
4.1 Discussion for the spargers.....	30
4.2 Conclusions .....	30
5 References.....	32
6 Remaining documentation .....	33

## List of Tables

Table 1. Mathematical description of the different individual forces acting on a bubble and their dependences. $\sigma_L$ : surface tension in [N/m], $\Delta P$ : capillary pressure in [Pa], $r_p$ : pores radius in [m], $F_d$ : drag force in [N], $\rho_L$ : liquid density in [kg/m <sup>3</sup> ], $W$ : average velocity of bubble expansion in [m/s], $\pi$ : universal constant “pie”, $d_b$ : bubble diameter in [m], $\mu_L$ : liquid viscosity in [Pa s], $F_s$ : surface tension force in [N].(Kazakis, Mouza and Paras, 2008). ....	8
Table 2. Calibration data for the air-flow meter used for the trials. ....	33

## List of Figures

Figure 1. Bubble formation through a pore of a porous material and forces acting on the bubble. ....	9
Figure 2. Sparger devices and sparger bodies. For the cylindrical plastic sparger, the red line corresponds to the point that the sparger was shorten (iii). The underlined porous disk (on the right) was not used, the middle one corresponds to sparger iv, (porous size: X1) and the one on the left is the fine porous (porous size: X2) disk (v). The fine disk (porous size: X3) on the left was also glued (vi) in the support used. The highlighted support materials that accept one and two disks were used for the trials involving porous disks.....	10
Figure 3. Picture on the left: airflow meter, the read is done using the metallic ball, the reading is translated into airflow using Table 1 (in Appendix) or Figure 4. Picture on the right is the SUB with the L-shape tubes, the metallic sparger and one of the single use spargers.....	10
Figure 4. Air flow based on the ball location in the flow-meter.....	11
Figure 5. Bubbles generation through different spargers at air inlet flowrate 21.81 ccm. (i) metallic sparger, (ii) cylindrical single use sparger, (iii) porous disk X2, (iv) porous disk X3, (v) porous disk X3 glued, (vi) porous disk X2 in sparger body for two, and (vii) porous disk X2 in sparger body for three.....	14
Figure 6. Bubbles generation through different spargers at air inlet flowrate 29.65 ccm. (i) metallic sparger, (ii) cylindrical single use sparger, (iii) cylindrical single use sparger with shorten connection, (iv) porous disk X2, (v) porous disk X3, (vi) porous disk X3 glued, (vii) porous disk X2 in sparger body for two, and (viii) porous disk X2 in sparger body for three. ....	15
Figure 7. Bubbles generation through different spargers at air inlet flowrate 38.97 ccm. (i) metallic sparger, (ii) cylindrical single use sparger, (iii) cylindrical single use sparger with shorten connection, (iv) porous disk X2, (v) porous disk X3, (vi) porous disk X3 glued, (vii) porous disk X2 in sparger body for two, and (viii) porous disk X2 in sparger body for three. ....	17
Figure 8. Bubbles generation through different spargers at air inlet flowrate 49.98 ccm. (i) metallic sparger, (ii) cylindrical single use sparger, (iii) porous disk X2, (iv) porous disk X3, (v) porous disk X2 in sparger body for two, and (vi) porous disk X2 in sparger body for three.....	18
Figure 9. Bubbles generation through different spargers at air inlet flowrate 62.98 ccm. (i) metallic sparger, (ii) cylindrical single use sparger, (iii) porous disk X2, (iv) porous disk X3, (v) porous disk X2 in sparger body for two, and (vi) porous disk X2 in sparger body for three.....	19
Figure 10. Bubbles generation through different spargers at air inlet flowrate 78.20 ccm. (i) metallic sparger, (ii) cylindrical single use sparger, (iii) porous disk X2, (iv) porous disk X3, (v) porous disk X2 in sparger body for two, and (vi) porous disk X2 in sparger body for three.....	19
Figure 11. Bubble formation through a sparger body with for 2 disks (porous size 15 $\mu$ m). The pictures were taken at consecutive time intervals.....	20
Figure 12 Bubble generation through disk sparger.....	20
Figure 13. Bubble coalesce and bubble generation through the joint areas.....	21

Figure 14. Bubble coalesce.....	21
Figure 15. Comparison of the straight tube with a plastic sparger attached on it (a.) no modification in the design and (b.) metallic sparger on L-shaped tube flow rate location 20cm. ....	22
Figure 16 Comparison of the straight tube with a plastic sparger attached on it (a.) no modification in the design and (b.) metallic sparger on L-shaped tube flow rate location 20cm. ....	22
Figure 17. Comparison of the straight tube with a plastic sparger attached on it (a.) no modification in the design and (b.) metallic sparger on L-shaped tube flow rate location: 60cm. ....	22
Figure 18. Bubble generation at very low air flowrate. (a) two orifices and (b) three orifices. Flowrate: <10mm (ball location). ....	23
Figure 19. Bubble generation. (a) two orifices and (b) three orifices. Flowrate=10mm (ball location). ....	23
Figure 20. Bubble generation. (a) two orifices and (b) three orifices. Flowrate: 20mm (ball location). ....	24
Figure 21. Bubble generation. (a) two orifices and (b) three orifices. Flowrate: 30mm (ball location). ....	24
Figure 22. Bubble generation. (a) two orifices and (b) three orifices. Flowrate: 40mm (ball location). ....	24
Figure 23. Bubble generation. (a) two orifices and (b) three orifices. Flowrate: 50mm (ball location). ....	25
Figure 24. Comparison of the straight tube with a plastic sparger attached on it (a. no modification in the design, b. sparger glued on the tube). Flow rate location: 20cm. ....	27
Figure 25 Comparison of the straight tube with a plastic sparger attached on it (a. no modification in the design, b. sparger glued on the tube). Flow rate location: 40cm. ....	27
Figure 26. Comparison of the straight tube with a plastic sparger attached on it a. no modification in the design, b. sparger glued on the tube. Flow rate location: 60cm.....	27
Figure 27. Current design of the plastic sparger. It consists of 2 main parts, a sparger body and the main sparger connected to the sparger body. The main sparger body is cylindrical in shape, made from porous material and there is a flat surface at the end of the cylinder. ....	28
Figure 28. <b>Proposed design 1:</b> it consists of one sparger body made of plastic porous material, threating with a plastic orifine have been used for the effective connection without losses with the air tube. The surface at the end of the sparger has not been modified from flat but the mass transfer resistance has been increased by increasing the distance between the tube and the end surface. ....	28
Figure 29. <b>Proposed design 2:</b> it consists of one sparger body made of plastic porous material, threating with a plastic orifine have been used for the effective connection without losses with the air tube. The surface at the end of the sparger has been modified from flat to more “roundish” and the mass transfer resistance has been increased by increasing the distance between the tube and the end surface. ....	29

Figure 30. Evaluation of the new design (flat area has not yet improved). Flowrates at ball location:  
a. 20, b. 40, c. 60 and d. 70mm. ....29

# 1 Short introduction

A very important process for the majority of bioprocesses is the supply of oxygen to the medium that is required for the growth, maintenance and the metabolic production of the microorganisms in cell cultures (Garcia-ochoa and Gomez, 2009). Usually, the aeration in cell culture bioreactors is performed by bubble aeration, bubble-free aeration or indirect aeration (Czermak *et al.*, 2005). Bubble aeration methods, which are commonly used in industrial applications because they are characterized by high oxygen mass transfer in water due to high volume specific phase surface. However, using this method may damage the sensitive cells due to shear stress forces developed when bubbles penetrate the surface and burst. Using bubble aeration, foam is generated on the surface of the culture resulting medium reduction of medium in the reactor (Czermak *et al.*, 2005). Bubble free aeration systems might be ideal to control the bubble size distribution creating small bubbles and avoid damaging cell by avoiding the development of shear stress forces (Cote, Jean-Luc and Huyard, 1989; Ducommun *et al.*, 2000). However, the surface of the membranes should be high enough for in order to achieve sufficient oxygen supply to the medium. The latter might lead to costly installations which are difficult to maintain and it might be problematic, where a sterile environment for the production is desired (Czermak *et al.*, 2005). Other aeration systems like vortex aeration (Chisti and Moo-Young, 1993), spiral liquid flow microbubble generator (Terasaka *et al.*, 2011), mechanical vibration, flow focusing, fluidic oscillation (Zimmerman *et al.*, 2008), spin filters, vibro mixers, have also been reported, however, the installation cost is prohibited for a production facility (Czermak *et al.*, 2005).

The mass transfer rate usually depends on physico-chemical properties of the liquid, the sparger design, the diameter of the orifice or the porous size, the tank design, impeller, air flowrate and the presence of a chemical reaction (Martín, Montes and Galán, 2008). Important factors for the efficient oxygen mass transfer from the bubble to the medium is the bubble size and the uniformity of bubble size distribution. Large bubbles have smaller interfacial area which means lower mass transfer rates and lower residence time in the bioreactor. The formation of large bubbles provides an inefficient oxygen supply, increased aeration cost and high probabilities of cell damage. On the other hand, smaller bubbles offer higher interfacial area and therefore higher mass transfer flux and higher residence times, which preventing cell damage and improving oxygen utilization. The initial bubble size depends on the distance between the orifices or the porous size, which might prevent from possibilities of bubble coalescing and liquids with low surface tension, which exhibits no tendency for coalescing (Kazakis, Mouza and Paras, 2007). Bubble size is an important design parameter since it dictates the available gas-liquid mass transfer interfacial area (Kazakis, Mouza and Paras, 2008). Phenomena like coalescing and breakage occur directly onto the sparger surface or in the vicinity of the sparger surface, therefore, it is essential to know the initial bubble size distribution after the detachment from the sparger for various gas-liquid systems (Kazakis, Mouza and Paras, 2008) and different sparging systems.

## *Bubbles formation and detach*

When bubbles are formed through an orifice or aperture, the liquid attached to the perimeter of the orifice serves as an anchor as the wetting force attaches the growing bubble to the solid surface. The bubble will grow until the point that the buoyant force on the bubble (which is a function of the bubble volume) exceeds the anchoring restraint on the bubble (typically proportional to contact perimeter) and it will detach the surface. Only if the anchoring force is disrupted, the bubble can also break-off earlier (Zimmerman *et al.*, 2008). The material properties (wetting properties) have a significant role here as a hydrophobic material will form a second anchor force on the bubble, which will require a larger volume to overcome, on the other hand, when a hydrophilic material is used the extra anchoring

forces are not there (Zimmerman *et al.*, 2008). A schematic representation of the bubble formation through a pore is illustrated in Figure 1 where the forces acting on the bubble are also illustrated. The initial size of the bubble will certainly depend on size of the forces acting on the bubble, higher downward forces will require higher upward forces. According to (Kazakis, Mouza and Paras, 2008), the initial bubble size distribution depends on the (a) porous diameter, (b) gas flow, (c) viscosity and (d) surface tension. Small and numerous bubbles are generated through the small pores, this is explained if one considers two systems with the only difference the **porous size**, one has large and the other one smaller. In both systems the downward forces are the same but the pressure required to form a bubble for a bigger pore is lower than the pressure required for a smaller pore, that makes the bubble formation easier and as the bubble escaping very easy not all the pores are activated. The bubble starts to form on a pore when the pressure under the chamber increases due to air flow and overcomes the capillary pressure. Another parameter that determines the initial bubble size is the **gas flow rate**, when it is low, only some pores are activated and produce larger bubbles, however, when a higher flowrate is applied; more pores, even smaller ones, are activated providing smaller bubbles. This phenomenon might also be resulted due to higher upward forces which attributed to gas momentum. **Viscosity** is another variable important for the initial bubble size higher viscosity leads to smaller bubble size distribution. The viscosity influences the drag force, for liquid with higher viscosity the drag force is higher so the formation of a big bubble is difficult to be achieved. Finally, the force that depends on **surface tension** is the one that “holds” the bubble on the sparger’s surface, therefore lower surface tension leads to lowers sizes. Table 1 lists the mathematical description of each variable and the corresponding force.

Table 1. Mathematical description of the different individual forces acting on a bubble and their dependences.  $\sigma_L$ : surface tension in [N/m],  $\Delta P$ : capillary pressure in [Pa],  $r_p$ : pores radius in [m],  $F_d$ : drag force in [N],  $\rho_L$ : liquid density in [kg/m<sup>3</sup>],  $W$ : average velocity of bubble expansion in [m/s],  $\pi$ : universal constant “pie”,  $d_b$ : bubble diameter in [m],  $\mu_L$ : liquid viscosity in [Pa s],  $F_s$ : surface tension force in [N]. (Kazakis, Mouza and Paras, 2008).

Description	Equation	Comment
Capillary pressure	$\Delta P = \frac{2\sigma_L}{r_p}$	Pressure difference decrease with increasing porous diameter
Drag force	$F_d = \frac{1}{2}\rho_L W^2 \frac{\pi d_b^2}{4} \left( \frac{24\mu_L}{\rho_L W d_b} + 1 \right)$	Drag force increase with increasing viscosity $\mu_L$
Surface tension force	$F_s = 2\pi r_p \sigma_L$	Increasing surface tension, force is increasing

The **sparger material** has been reported to have a significant contribution on bubbles formation as it affects the contact angle, however, as it has been tested using numerous materials as glass, stainless steel, Teflon and nickel only Teflon does not have a significant effect on bubbles formation and it behaves as stainless steel that is commonly used. Properties of the sparger material, or the medium and physico-chemical properties are not the only things to be considered but also phenomena that take place onto or very close to the sparger surface such as breakage and coalescing are having an important role on bubble formation (Kazakis, Mouza and Paras, 2008).

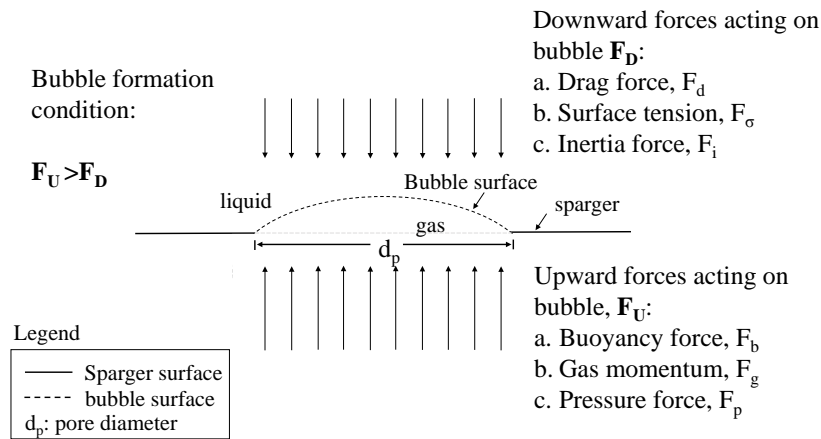


Figure 1. Bubble formation through a pore of a porous material and forces acting on the bubble.

To cultivate cell cultures bioreactors made from glass and steel were commonly used. However, for these kind of processes, which are used for the production of pharmaceutical products such as antibodies or biosimilars, sterilization is an important parameter as proper cleaning procedures and validation prevents product contamination and therefore, a successful batch production. The cleaning procedure now, is a time consuming process that requires a lot of utilities like the use of solvents, a lot of water, steam and energy and the risk of product contamination is always possible. The single use requirement is pre-sterilized while the supplier is responsible for the quality assurance, the single-use bioreactors are ready to be used savings a lot of valuable time by avoiding all the cleaning procedures. Therefore, single use technology is a valuable innovation for the pharmaceutical industry and the multipurpose production facilities as it eliminates the risk of equipment contamination, provides saving with respect to time and utilities maximizing at the same time the number of batches per year. An important limitation of such a technology is the scalability as the achievable oxygen transfer rates depend on the maximum tolerated pressure, energy transfer of the mixing system consisting of impellers and spargers and insulating the plastic material reduces the efficiency of heat transfer (Schmidt, 2017).

In this project, the effect of different types of spargers on the formation of bubbles, the bubble size distribution and the bubble size is to be examined. The objective of this study, is to investigate and evaluate the possibilities to replace a commonly used porous steel sparger attached on an L-shaped tube with a single use plastic sparger attached on straight tube. Therefore, the challenge here is, to imitate the bubble size distribution and the bubble size that is generated by a stainless steel sparger on an L-shaped tube by using a single-use plastic sparger on a straight tube. To achieve the above-objective, first, an evaluation of the available single-use spargers and a comparison with the steel sparger under different process conditions (e.g. air flow-rate) are performed. From the analysis of the different testings, possible material weaknesses to generate narrow bubble size distribution and small bubbles are identified, suggestions to improve those weaknesses are made, and new designs are proposed and finally, validated through experimental trials.

## 2 Materials and methods

The spargers described above as well as the sparger bodies for porous disk spargers are illustrated in Figure 2.

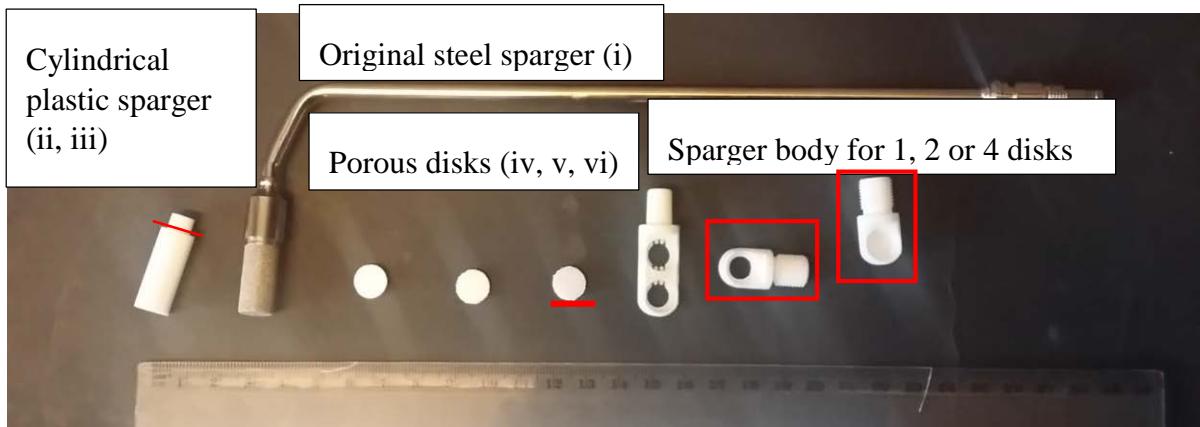


Figure 2. Sparger devices and sparger bodies. For the cylindrical plastic sparger, the red line corresponds to the point that the sparger was shorten (iii). The underlined porous disk (on the right) was not used, the middle one corresponds to sparger iv, (porous size: X1) and the one on the left is the fine porous (porous size: X2) disk (v). The fine disk (porous size: X3) on the left was also glued (vi) in the support used. The highlighted support materials that accept one and two disks were used for the trials involving porous disks.

The airflow meter as well as the single use bioreactor with the L-shaped tubes are depicted in Figure 3.

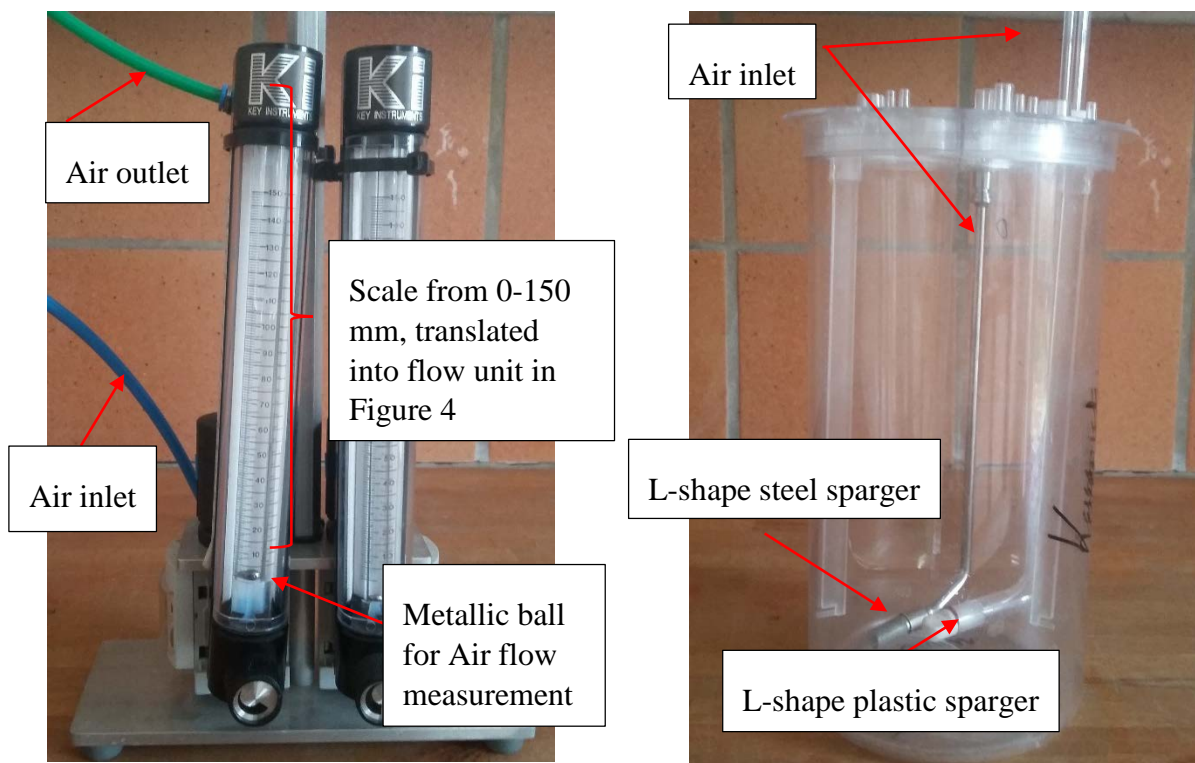


Figure 3. Picture on the left: airflow meter, the read is done using the metallic ball, the reading is translated into airflow using Table 1 (in Appendix) or Figure 4. Picture on the right is the SUB with the L-shape tubes, the metallic sparger and one of the single use spargers.

## 2.1 Airflow calibration

Based on calibration data provided by the manufacturer, the flow of the air depending of the ball position in the flow meter is illustrated in Figure 4 (the data points are given in Table 1 in Appendix).

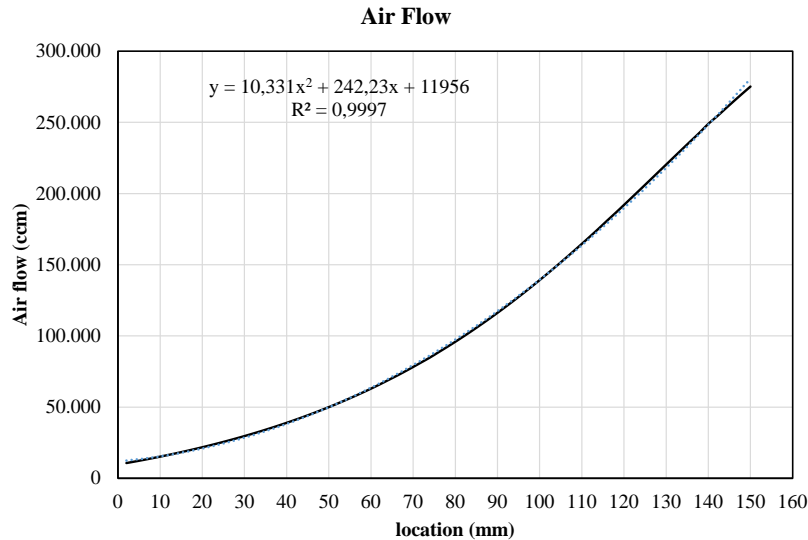


Figure 4. Air flow based on the ball location in the flow-meter.

## 2.2 Method

A systematic method to decompose the problem into sub-problems in order to evaluate different designs, identify weaknesses and suggest improved designs is proposed. The method consists of five steps which are listed below. The main tool for performing the steps and collecting information is experimentation.

**Step 1.** Problem definition: In this step, the main objectives of the study are defined in a clear manner.

**Step 2.** Testing: In this step, different testing alternatives are defined.

**Step 3.** Evaluation and identification: In this step, the results obtained using step 2 are analysed and evaluated. Then, weaknesses of equipment are identified and documented.

**Step 4.** Suggestions and testing: In this step, suggestion based on the identified equipment weaknesses are made for new design which is tested.

**Step 5.** Application: Once the testing of the new design is successful the new design might be applied in a real system for the final validation.

## 3 Results

In this section, the application of the method is illustrated and each step has been tackled detailed and analytically.

### 3.1 Step1. Problem definition

An aeration system made of plastic attached on a straight tube for single use bioreactors (SUB) that provides the same, similar or better bubble size and size distribution compared to the originally sparger attached on L-shape tube used in glass-steel bioreactors is to be investigated.

### 3.2 Step 2. Testing

To achieve the main objective of this project, first, the available equipment needs to be tested and possible weaknesses, if any, to be identified and finally, a new design, if needed, to be proposed. The tests required to achieve the objective are listed below.

**Test 1.** Evaluate the bubble size distribution in bioreactors using different sparger types (see Figure 2) attached on L-shaped tube under different inlet air flow rates:

- i. Original steel sparger
- ii. Cylindrical plastic
- iii. Cylindrical plastic with shorten connection
- iv. Sparger body for one side disk (porous size, 15  $\mu\text{m}$ )
- v. Sparger body for one disk (porous size, 100  $\mu\text{m}$ )
- vi. Sparger body for one disk, glued (porous size, 100  $\mu\text{m}$ )
- vii. Sparger body for 2 disks (porous size, 15  $\mu\text{m}$ )
- viii. Sparger body for 2 disks (porous size, 100  $\mu\text{m}$ )

**Test 2.** Evaluate bubble generation and coalesce phenomena.

**Test 3.** Evaluate bubble generation through straight tube for different configuration of the cylindrical sparger and compare with the metallic sparger.

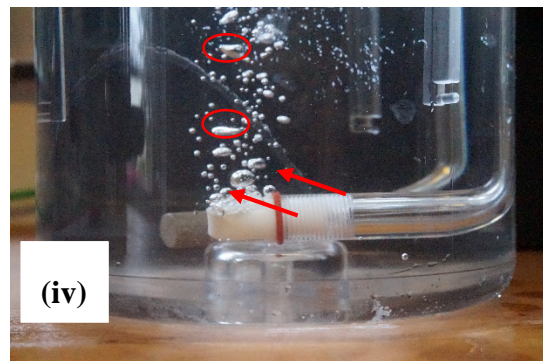
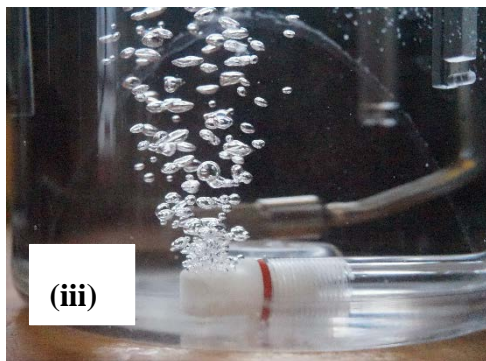
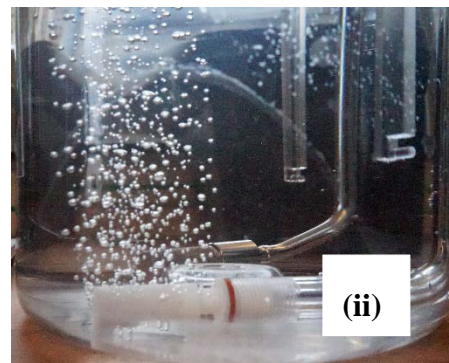
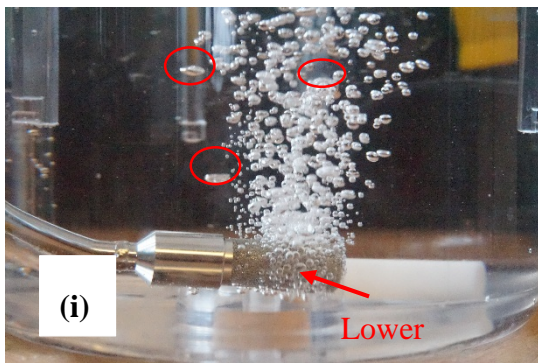
**Test 4.** Bubble generation through non-porous material with 2 and 3 orifices.

### 3.3 Step 3. Evaluation and identification

*3.3.1 Test 1. Evaluate the bubble size distribution in bioreactors using different sparger types attached on L-shaped tube.*

In Figure 5, bubble generation through different spargers (i., ii., iii., iv., and v.) is depicted. It can be seen that, the steel sparger (see Figure 5i) provides relatively uniform small bubble-size distribution. There are, however, some bubbles (as the ones which have been highlighted) larger than the rest. This phenomenon might be the result of higher forces required for the bubbles to be released from the sparger's surface, especially, when they are formed in the lower surface (indicated in Figure 5i) of the sparger. Also, larger bubbles are possibly formed due to bubble coalesces during bubble formation near the sparger's surface. In Figure 5ii, bubbles generated by a cylindrical plastic sparger (single use sparger) are illustrated and it can be seen that the generated bubbles are in general small with narrow size distribution with only few bigger bubbles which might be the result of coalescing phenomena occurring in the system. Figure 5iii-vii, show bubble generation through porous disks. It can be seen

that the porous disk with porous size X2 (see Figure 5iii) generates, in general, big bubbles with wide size distribution, the same is seen for the fine disk used as the porous sparger in Figure 5iv. However, if one takes a closer look in Figure 5iv, the generated big bubbles are mainly result of air escaping from the void spaces around the sparger's perimeter, where the disk and the body sparger are connected and not through the porous material as it is supposed to be (shown in Figure 5iv with red arrows). This event affects the uniformity of the bubbles because, first, the bubbles are formed through irregular size voids and second, there is higher possibility that bubbles will coalesce during or after their formation on the porous disk because the bubbles are formed very close to each other. On the other hand, if the perimeter of the disk is sealed (e.g. glued) the air is forced to go through the porous material and it cannot go through the perimeter resulting a very narrow bubble size distribution (see Figure 5v.). In Figure 5vi and Figure 5vii, the use of two porous disks (porous size X2 and X3 respectively) in a body sparger for two disks is illustrated. The positioning of the sparger body is discussed in the second part (Test 2) of this section. It can be seen that the airflow through the void spaces and the growing mechanism have an important role in bubble formation and affect the initial bubble size uniformity. It can also be seen that the possibilities of bubbles coalescing when the bubbles are generated by vertical surfaces are high. This might be the result of the airflow through the void spaces, leading to decreased pressure, which increases the residence time of the bubbles on the surface of the porous material. Increased residence time means that (a) in the event that another bubble is formed close to the initially formed bubble, they might coalesce and (b) a formed bubble becomes larger in size in order to detach the sparger surface as the contribution of the gas momentum and pressure in the upwards forces are not sufficient (see Figure 5vi). Using the fine porous size disk (see Figure 5vii) some of the formed bubbles have actually smaller sizes, however, big bubbles resulting from coalescing phenomena are also noticed. It is interesting to investigate, the effect on the bubble size distribution when the void spaces around the disk are sealed.



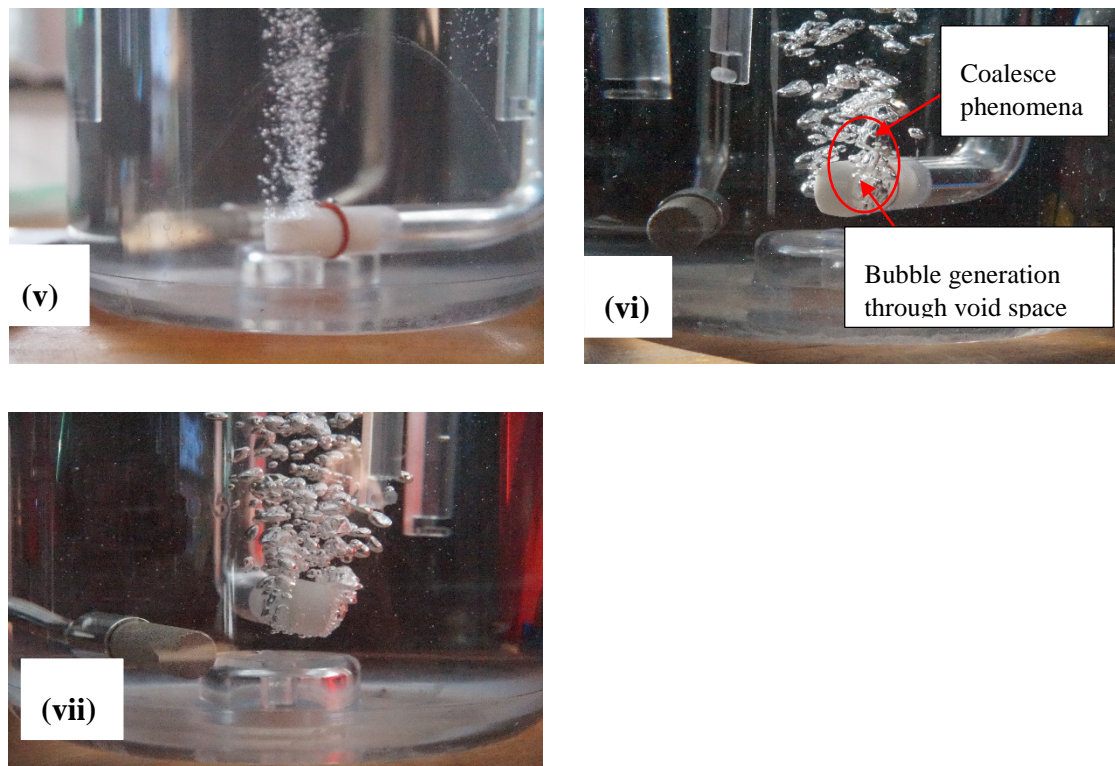


Figure 5. Bubbles generation through different spargers at air inlet flowrate 21.81 ccm. (i) metallic sparger, (ii) cylindrical single use sparger, (iii) porous disk X2, (iv) porous disk X3, (v) porous disk X3 glued, (vi) porous disk X2 in sparger body for two, and (vii) porous disk X2 in sparger body for three.

In Figure 6, similar observations for a slightly higher air inlet flowrate are made. Figure 6i-ii, illustrate the bubble-size distribution from the stainless steel sparger and the single-use plastic cylindrical sparger. It can be observed that the generated bubbles from these two spargers have uniform small size with only some small variations (as it is highlighted). In Figure 6iii, the same plastic cylindrical sparger has been used with the only difference being that the connection is shorten. The sparger produces a fine bubble-size distribution with some exceptions, especially in the connection part where the generated bubble size distribution is not uniform. This might be due to air losses created in the shorten connection surface. In Figure 6iv-v, it can be seen that the generated bubbles have different sizes with wide bubble size distribution due to bubble coalesces and possible, because of air flow through the perimeter of the disk. The later assumption has been evaluated by using a glued disk (see Figure 6vi), where it can be seen that forcing the air to go through the porous surface and not through the surrounding might have significant advantages. Similarly to the observations made for Figure 5vi and Figure 5vii, the airflow through the voids and the coalescing phenomena (see Figure 6vii and Figure 6viii) have an important role in bubble size.

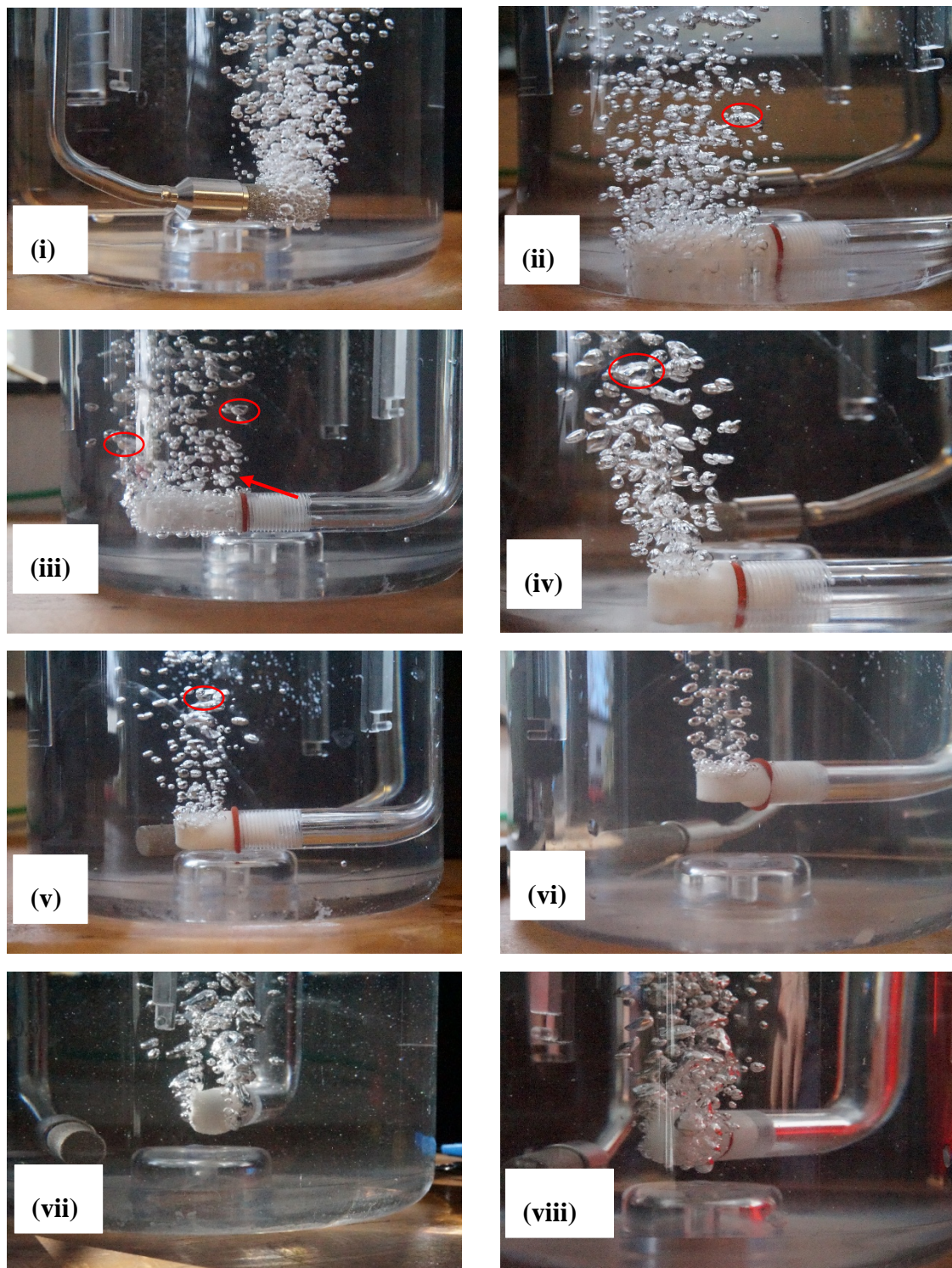
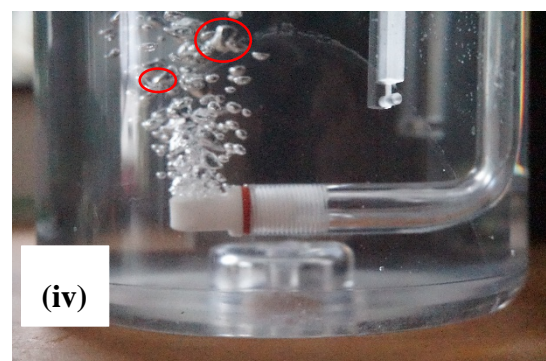
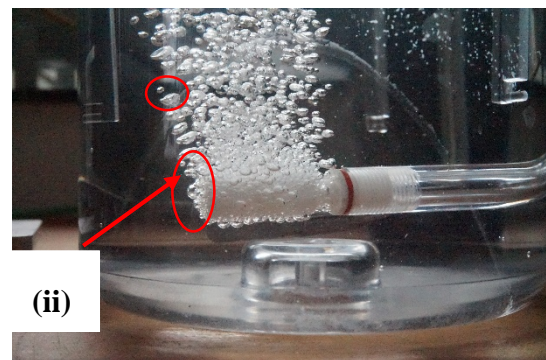
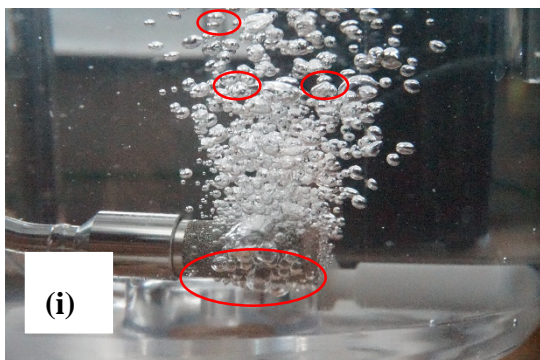


Figure 6. Bubbles generation through different spargers at air inlet flowrate 29.65 ccm. (i) metallic sparger, (ii) cylindrical single use sparger, (iii) cylindrical single use sparger with shorten connection, (iv) porous disk X2, (v) porous disk X3, (vi) porous disk X3 glued, (vii) porous disk X2 in sparger body for two, and (viii) porous disk X2 in sparger body for three.

In Figure 7, the bubble size distribution from different spargers is evaluated at higher inlet air flow rate (38.97 ccm). In general, similar trends, as in Figure 5-Figure 6, are observed. However, some larger bubbles are noticed when the steel sparger is used (Figure 7i). These larger bubbles might be

due to the higher forces required for the bubble to detach the lower part of the sparger surface which leads to possibilities for two bubbles to coalesce or larger bubbles. In Figure 7ii, it is seen that the plastic sparger produces narrow bubble size distribution with relatively small size, however, at the edges of the sparger some bubbles are quite larger than the ones generated from the main part of the sparger. This might be because of bubbles coalescing (see Figure 7ii). The cylindrical plastic sparger produces a good bubble size distribution, but, there are some larger bubbles produced on the surface of the sparger. In Figure 7iii, a sparger with shorten connection is illustrated and considering that the only difference with the sparger (ii) is that the connection is shorten (manually), the larger bubbles might not only be results of bubble coalesce, but possibly, because of pressure losses created in the connection of the sparger with the plastic tube, which might result longer bubble residence times on the porous surface and due to no sufficient pressure the bubbles need to become larger to overcome the buoyance force required to detach the surface. In Figure 7iv-v, it is obvious that the porous disks are not performing very well with respect to bubble size distribution that it is highly possibly due to air losses in the interfacial area between the disk and the sparger body. This assumption is supported by comparing Figure 7v and Figure 7vi, where the interfacial area between the disk and the support is glued. In Figure 7vi, it is seen that the generated bubbles have better size distribution than the ones presented in Figure 7v and the size of the bubbles are relatively small. A more interesting discussion might be resulted when more effective (non-soluble in water) glue on the joint points is going to be used. In Figure 7vii, at higher air flowrate, the generated bubbles are large without a uniform bubble size (similarly to the earlier observations), however, an improvement using the fine porous size disks (see Figure 7viii) can be achieved. In general, small bubbles with uniforms size distribution seems to be generated and the bigger ones seems to be result of the airflow through the void spaces.



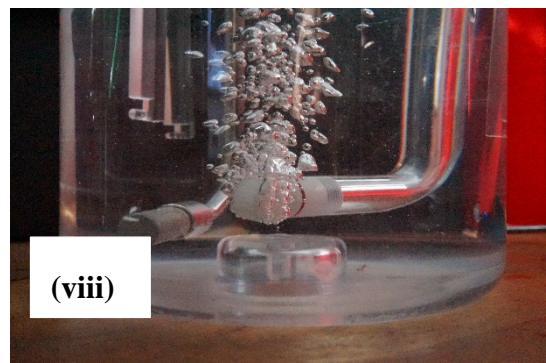
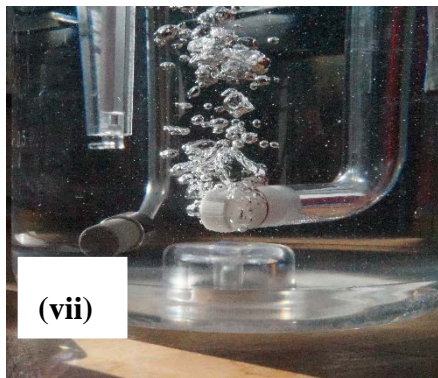
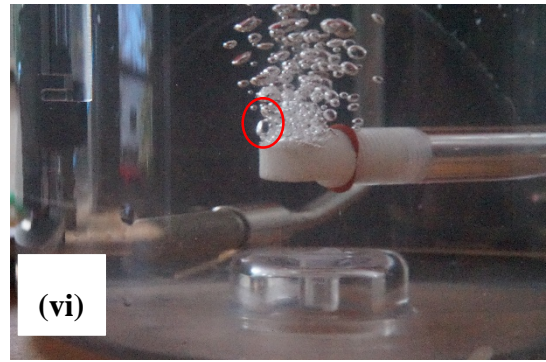


Figure 7. Bubbles generation through different spargers at air inlet flowrate 38.97 ccm. (i) metallic sparger, (ii) cylindrical single use sparger, (iii) cylindrical single use sparger with shorten connection, (iv) porous disk X2, (v) porous disk X3, (vi) porous disk X3 glued, (vii) porous disk X2 in sparger body for two, and (viii) porous disk X2 in sparger body for three.

At higher inlet air flowrates (Figure 8-Figure 10), it is noticed that the bubble size distribution generated by the cylindrical plastic sparger (see Figures 5ii-7ii) is much better compared to other tested spargers. The steel sparger generates a good bubble-size distribution, but sometimes larger bubbles are noticed (Figures 5i-7i). The porous disk spargers generate non-uniform bubbles, mainly because of the air losses in the interfacial area between the disk and the support (see Figure 8iii, iv, v, vi -Figure 10iii, iv, v, vi).



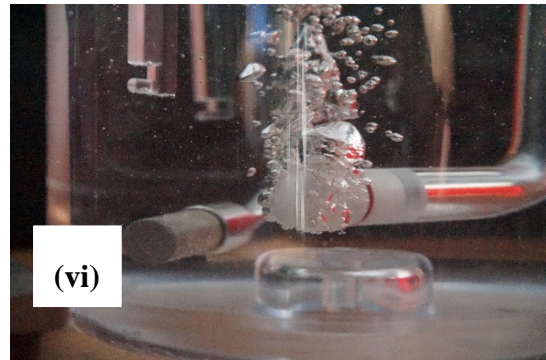
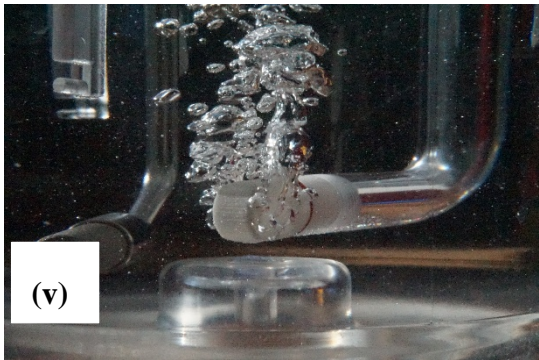
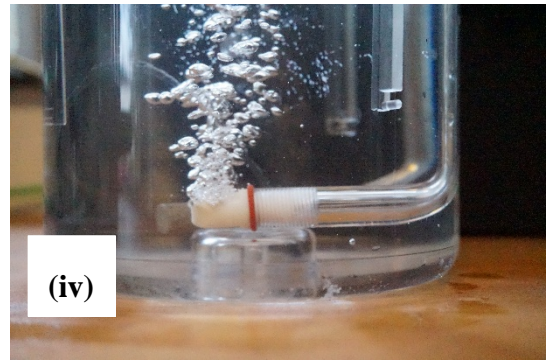
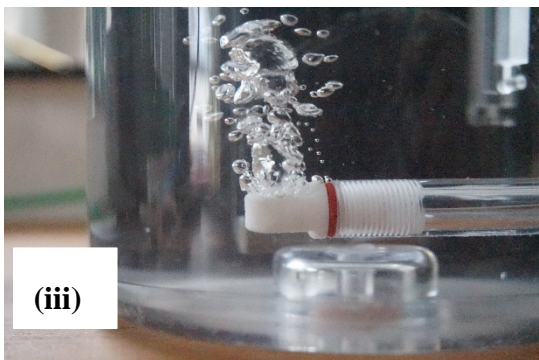
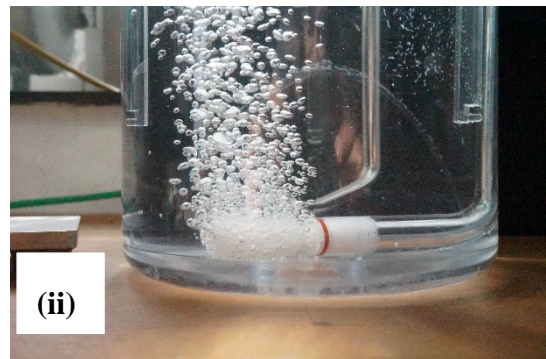


Figure 8. Bubbles generation through different spargers at air inlet flowrate 49.98 ccm. (i) metallic sparger, (ii) cylindrical single use sparger, (iii) porous disk X2, (iv) porous disk X3, (v) porous disk X2 in sparger body for two, and (vi) porous disk X2 in sparger body for three.



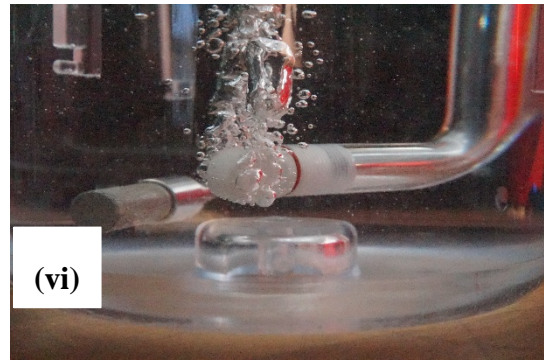
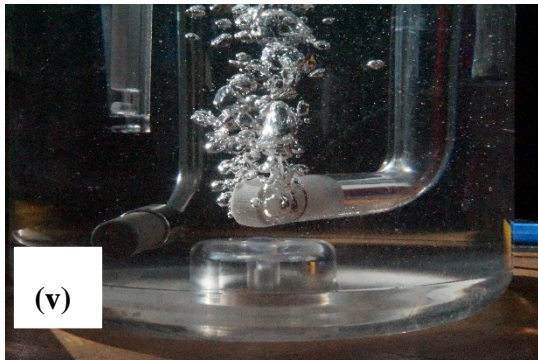


Figure 9. Bubbles generation through different spargers at air inlet flowrate 62.98 ccm. (i) metallic sparger, (ii) cylindrical single use sparger, (iii) porous disk X2, (iv) porous disk X3, (v) porous disk X2 in sparger body for two, and (vi) porous disk X2 in sparger body for three.

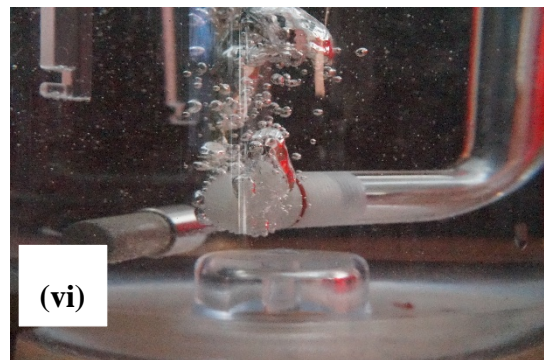
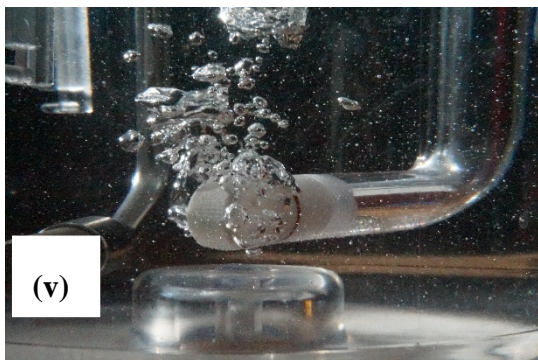
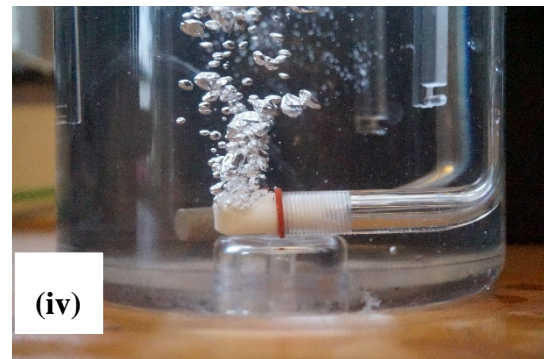


Figure 10. Bubbles generation through different spargers at air inlet flowrate 78.20 ccm. (i) metallic sparger, (ii) cylindrical single use sparger, (iii) porous disk X2, (iv) porous disk X3, (v) porous disk X2 in sparger body for two, and (vi) porous disk X2 in sparger body for three.

### 3.3.2 Test 2. Evaluate bubble generation and coalescing phenomena

In this section, the assumptions regarding the bubble generation through the void spaces and through the sparger surfaces facing at the bottom of the reactor are to be evaluated and discussed. In Figure 11, two pictures taken at time  $t$  and time  $t+\Delta t$  (consecutive time intervals) are illustrated. The sparger in Figure 11 consists of two disks (porous size  $15\ \mu\text{m}$ ) on a body sparger for two disks. It is clearly seen that bubbles generated in the lower surface have to be large enough in order to overcome the attractive forces to the surface and finally, to detach the surface of the sparger due to higher required buoyance force. Therefore, coalescing phenomena are likely to happen when bubbles are formed in the surface facing in the bottom of the bioreactor. This observation shows that if two large bubbles are formed, then they might have higher possibilities to coalesce and form an even larger bubble with irregular (or non-desirable) shape.

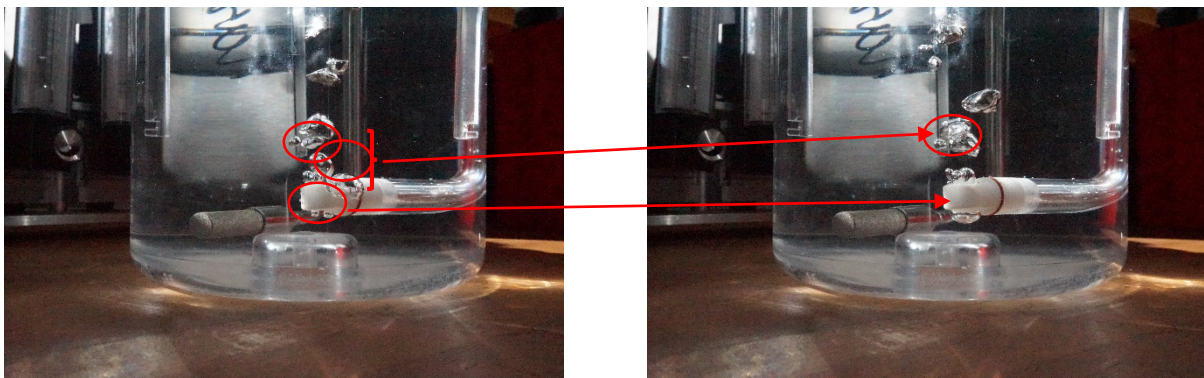


Figure 11. Bubble formation through a sparger body with for 2 disks (porous size  $15\ \mu\text{m}$ ). The pictures were taken at consecutive time intervals.

In Figure 12, bubbles generated at very low airflow are shown. It is seen that the generated bubbles do have different size, this is because one bubble is generated through the void space and therefore, has an irregular size and the other one through the porous material.

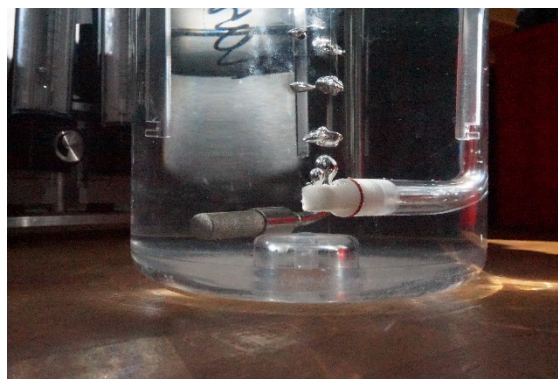


Figure 12 Bubble generation through disk sparger.

In Figure 13, the same sparger has been rotated  $90^\circ$ , to avoid bubble generation through the porous disk below the sparger. Here, the generation through the void spaces is illustrated as well as the bubble coalesce. A clearer look on bubble coalesce is illustrated in Figure 14.

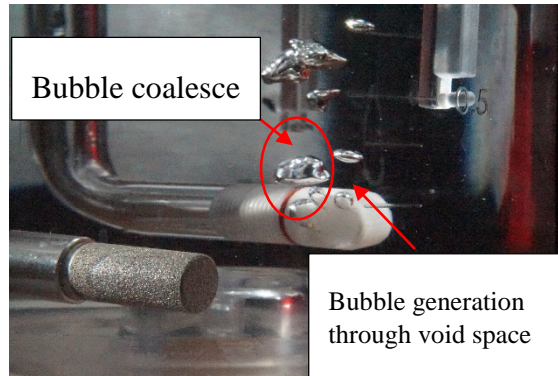


Figure 13. Bubble coalesce and bubble generation through the joint areas.



Figure 14. Bubble coalesce.

Concluding Test 2, several issues can be discussed such as the position of the porous disk, sealing the surroundings to force the air to go through the porous material and finally, to minimize the use of spargers that there is a possibility to generate bubbles below the sparger (especially for non-cylindrical material, like flat surfaces). The position of the sparger should be towards the upper surface of the reactor, otherwise phenomena resulting in larger bubbles as shown in Figure 13 and Figure 14 might take place. Moreover, the surroundings should be sealed, otherwise irregular size bubbles without having the right distance between them are generated. Finally, when the sparger is facing the upper surface, bubbles should not be generated from flat surfaces facing the bottom of the reactor because larger bubbles are formed due to forces required and leading as well, to higher possibilities of coalesce and collision phenomena.

### 3.3.3 Test 3. Comparison of a straight tube with cylindrical plastic sparger with an L-shaped tube with metallic sparger.

In Figure 15, the bubble formation through the same plastic sparger attached on a straight tube (see Figure 15a) compared with the metallic sparger on L-shaped tube (see Figure 15b) is depicted. It can be seen that, in general, the bubble size distribution as well as the bubble size is similar in comparison with the original one, however, there are some larger bubbles generated from the flat surface facing the bottom of the reactor similarly with the metallic sparger (see Figure 15b). In Figure 15a, it can be seen that bubbles are also generated through the connection points that lead to larger bubbles due to coalescing phenomena. Similar observations are noticed at higher air inlet flowrates as shown in Figure 16 and Figure 17.

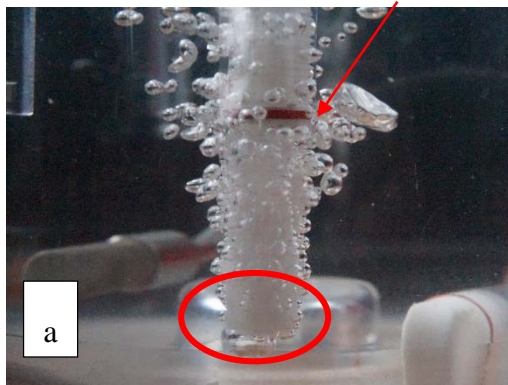


Figure 15. Comparison of the straight tube with a plastic sparger attached on it (a.) no modification in the design and (b.) metallic sparger on L-shaped tube flow rate location 20cm.



Figure 16 Comparison of the straight tube with a plastic sparger attached on it (a.) no modification in the design and (b.) metallic sparger on L-shaped tube flow rate location 20cm.



Figure 17. Comparison of the straight tube with a plastic sparger attached on it (a.) no modification in the design and (b.) metallic sparger on L-shaped tube flow rate location: 60cm.

From the analysis performed above, it is concluded that the plastic cylindrical sparger attached on a straight tube performs equally well with respect to bubble size distribution and bubble size when compared with the metallic sparger. However, to avoid the formation of larger bubbles, especially, the ones formed at the surface facing at the bottom of the reactor, another design to prevent or to minimize the air transfer through this flat surface needs to be proposed. Moreover, it had been seen that losses through joint areas are not particularly good for the bubble size distribution as through these joints irregular in size bubbles with high probabilities to coalesce are formed.

### 3.3.4 Test 4. Bubble generxation through non-porous material with 2 and 3 orifices (SIZE of orifices)

In large scale, bubble generation is usually taking place through orifices of non-porous material (usually steel). Using this design the generated bubbles are only going out from the orifices in a size depending on the air flowrate. In this section, the objective is to evaluate the bubble size generation through the described design and compare it with other previously tested porous spargers. In the following figures (see Figure 18-Figure 23), pictures of the non-porous spargers are illustrated. In Figure 18, the bubbles at very low air inlet flowrate are relatively large and unevenly distributed even though the orifices are very small. Figure 18 verified, the observed phenomenon (Zimmerman *et al.*, 2008) that the small bubbles do not depend on how small is the orifice. In Figure 18, it is as well noticed that the bubbles do not have a spherical shape after their detachment.

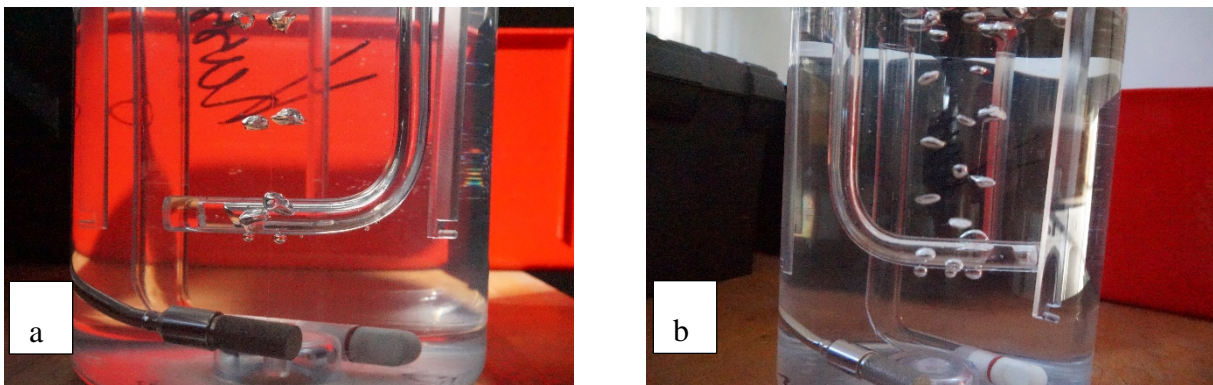


Figure 18. Bubble generation at very low air flowrate. (a) two orifices and (b) three orifices. Flowrate: <10mm (ball location).

In Figure 19-Figure 23 higher air flowrate has been used, and it can be noticed that in the cylinder with two orifices bubble coalescing takes place very early resulting to large bubbles with irregular shape and size. Similarly, bubbles generated through the cylinder with three orifices tend to coalesce at low air flowrate and at higher air flowrates they are coalescing more often creating larger bubbles. In general, these designs seems not useful unless a very low air flowrate is being used. In the latter case, the question of supplying adequate amount of oxygen in the systems arises.

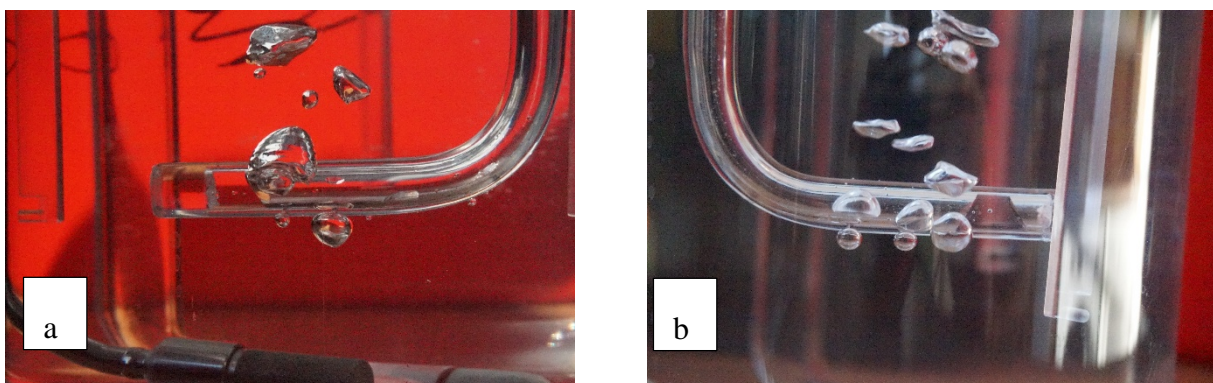


Figure 19. Bubble generation. (a) two orifices and (b) three orifices. Flowrate=10mm (ball location).



Figure 20. Bubble generation. (a) two orifices and (b) three orifices. Flowrate: 20mm (ball location).



Figure 21. Bubble generation. (a) two orifices and (b) three orifices. Flowrate: 30mm (ball location).



Figure 22. Bubble generation. (a) two orifices and (b) three orifices. Flowrate: 40mm (ball location).

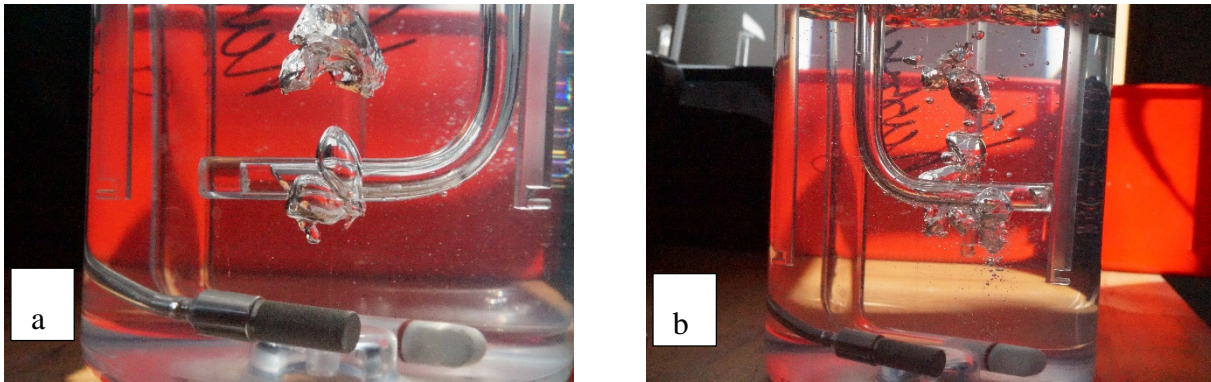


Figure 23. Bubble generation. (a) two orifices and (b) three orifices. Flowrate: 50mm (ball location).

### 3.3.5 Observations and discussion on bubble generation

In general, the plastic spargers are able to produce small bubbles, however, the bubble size distribution is not always narrow (especially for the porous disks). One of the main reasons that this phenomenon takes place is that the air does not always exit through the porous material but also through the connection points. This might affect the generated bubbles in the following three ways:

1. First, in order a bubble to be released from the surface, higher forces than the ones which attract the bubble on the surface should be developed. In the case that there are air losses, the forces resulting from the air velocity (gas momentum) and gas pressure are decreased and therefore, for a bubble to detach the sparger area a higher buoyance force is required. The buoyance force depends on the bubble diameter, therefore, larger bubbles needs to be formed.
2. Secondly, if bubbles are formed through the voids, in the connection parts where they are not supposed to be formed, the distance between the generated bubbles is not desired, and there is, therefore, higher probability of coalescing phenomena and bubbles formation with irregular sizes.
3. Finally, large bubbles are generated from surfaces facing towards the bottom of the reactor where the surface area is either flat or the surface tension of the material is high. In both cases, the bubbles need to grow in size so the buoyance force overcomes the attractive forces of the sparger on the bubble.

### 3.3.6 Possible solutions:

Based on the observations and the analysis reported in sections 3.3.1-3.3.4, the following solutions are proposed:

- i. Sealing all the connection parts and force the air to go through the porous material. A threating with an orifine or glue can be used to seal joint parts.
- ii. Create sparger that the attractive forces on the bubbles are lower or add additives (such as surfactants) or other liquids (such as solvents) to increase the viscosity of the medium which assist in formation of smaller bubbles. However, the latter solution must be checked with respect to the oxygen mass transfer as the application of a surfactant or another liquid might lower the oxygen mass transfer from the bubble to the bulk liquid.
- iii. Create oscillation on the sparger. The addition of an extra force, given the inlet flowrate will decrease the buoyance forces required for the bubble to be released. This will reduce the average size of the generated bubbles but it might also increase the operating cost.

- iv. Using a sparger that can accommodate two porous disks facing upwards without porous disk facing downwards might have an improvement in the distribution of the generated bubbles when porous disks .
- v. Re-design the spargers to avoid mass transfer through flat surfaces that might create large bubbles (e.g. flat surfaces facing towards the bottom of the reactor) by eliminating flat surfaces or increasing the mass transfer resistance for the flat surfaces.

### **3.4 Step. 4. Suggestions and testing**

One of the main identified weaknesses is the air escaping through the joints. To evaluate this suggestion the following test is performed.

- 1. Plastic sparger on straight tube
  - a. No modification
  - b. Glued with the tube

In Figure 24-Figure 26, the performance of the glued cylindrical sparger is compared with the cylindrical sparger with no modification. It can be seen that the phenomena of air escaping through the connection points have been eliminated, however, larger bubbles continue to be formed at the flat surface facing towards the bottom of the reactor.

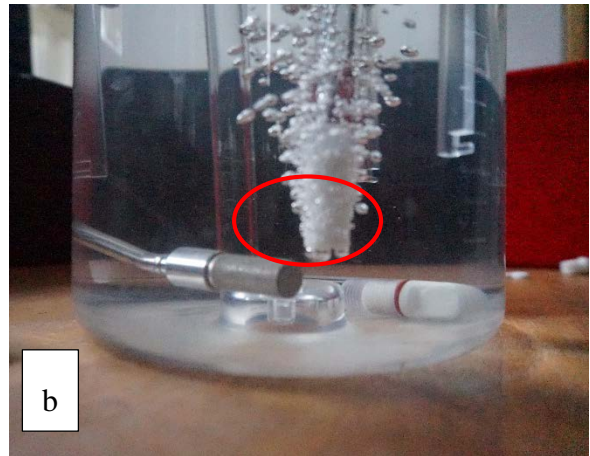
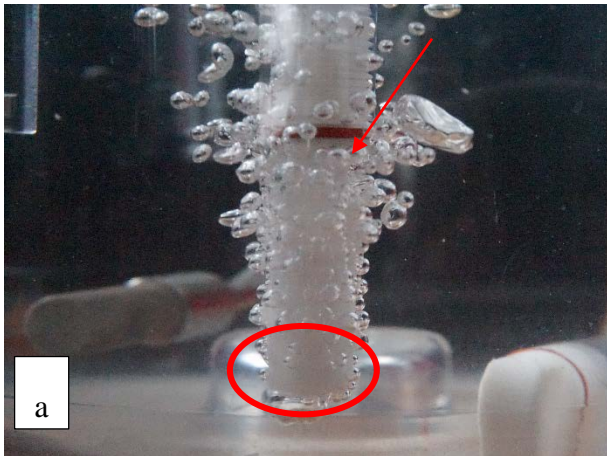


Figure 24. Comparison of the straight tube with a plastic sparger attached on it (a. no modification in the design, b. sparger glued on the tube). Flow rate location: 20cm.



Figure 25 Comparison of the straight tube with a plastic sparger attached on it (a. no modification in the design, b. sparger glued on the tube). Flow rate location: 40cm.



Figure 26. Comparison of the straight tube with a plastic sparger attached on it a. no modification in the design, b. sparger glued on the tube. Flow rate location: 60cm.

Considering the discussion for the limitations of the cylindrical plastic sparger when attached on straight shape tube a closer investigation of the current design is performed. In Figure 27, the current design of the plastic sparger is depicted, it consists of 2 main parts, the first small part is a sparger body that is screwed with the tube (air inlet) and sealed with (orifine) to avoid air losses. The other

part, the main sparger body is connected with the smaller one, in the joint there are some losses. Also at the end of the sparger the formed bubbles are quite large when the sparger is attached on a straight tube. This is because the formed bubbles require higher forces which depend on the bubble size to detach the sparger surface.

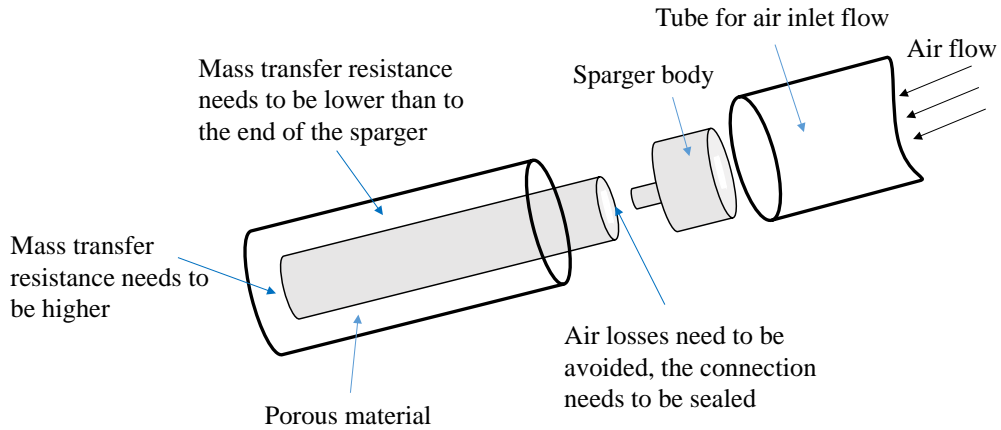


Figure 27. Current design of the plastic sparger. It consists of 2 main parts, a sparger body and the main sparger connected to the sparger body. The main sparger body is cylindrical in shape, made from porous material and there is a flat surface at the end of the cylinder.

The **proposed designs** taking into the considerations described before, are illustrated in Figure 28 Figure 29. The new designs, in both cases, consist of **one main sparger body** that is attached on a straight tube. This design will be sealed in the joint by creating a threading with an orifine, the distance between the inner tube (grey tube in Figure 28 and Figure 29) and the external surface will be increased so the mass transfer resistance of the boundary mass transfer resistance is increased and the surface at the end is going to be design in a round shape without sharp edges (Figure 29) and flat surface (Figure 28). The increased mass transfer resistance will make it difficult for the air to go through the end part of the sparger, and the later suggestion will make easier for bubbles to detach the surface as lower forces are applied on the formed bubble.

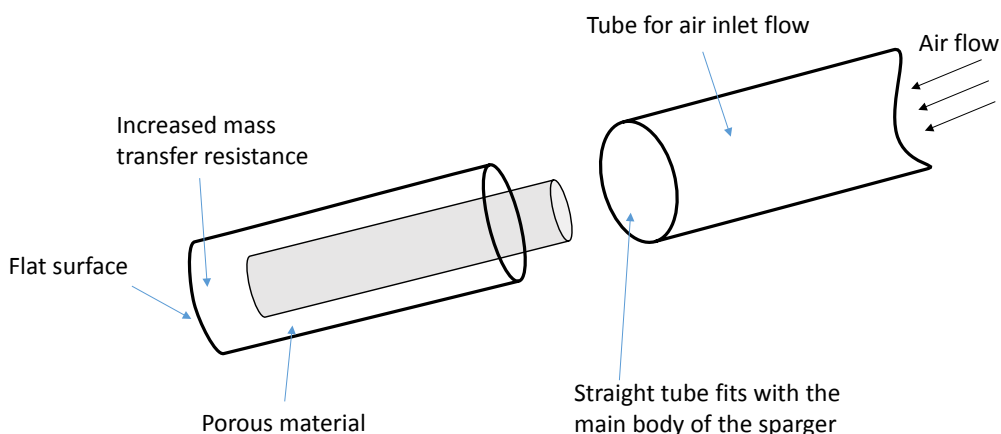


Figure 28. **Proposed design 1:** it consists of one sparger body made of plastic porous material, threading with a plastic orifine have been used for the effective connection without losses with the air tube. The surface at the end of the sparger has not been modified from flat but the mass transfer resistance has been increased by increasing the distance between the tube and the end surface.

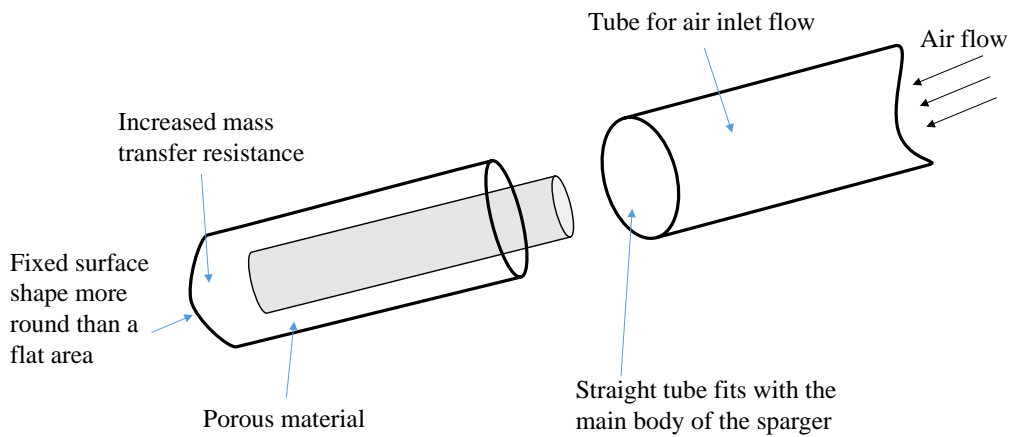


Figure 29. **Proposed design 2:** it consists of one sparger body made of plastic porous material, threading with a plastic orifine have been used for the effective connection without losses with the air tube. The surface at the end of the sparger has been modified from flat to more “roundish” and the mass transfer resistance has been increased by increasing the distance between the tube and the end surface.

In Figure 30, a first evaluation has been performed by sealing the joint points.

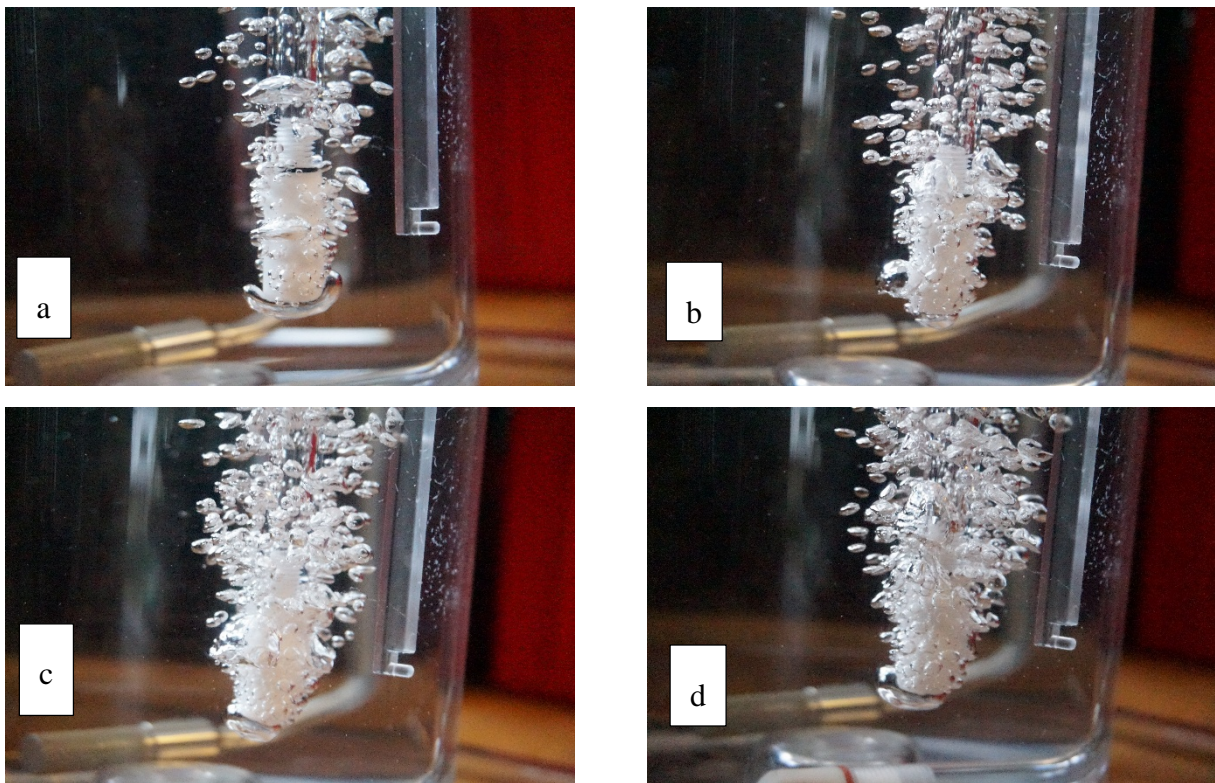


Figure 30. Evaluation of the new design (flat area has not yet improved). Flowrates at ball location: a. 20, b. 40, c. 60 and d. 70mm.

### 3.5 Step 5. Final Validation

This section will be completed once the new design is delivered.

## 4 Discussion and Conclusion

### 4.1 Discussion for the spargers

**Steel sparger:** At air-flowrates lower than 40ccm, the bubble size distribution is relatively narrow and the bubble sizes are in general small. The generation of larger bubbles might be because of high downward forces or the low upward forces acting on the bubble while the bubble is on the lower part of the sparger. Because of these forces and the pressure drop because the air is mainly released from the top, bubbles grow over time until the buoyancy forces becomes larger than the attractive forces of the surface material on the bubble and the bubble is detached from the surface.

**Cylindrical plastic sparger:** When a cylindrical plastic sparger is attached on L-shaped tube, the formed bubbles have uniform size distribution and small size with respect to different values of air inlet flowrate. During the tests, some larger bubbles have been noticed which are mainly generated at the connection points and at the end of the cylinder where the surface is flat. When a cylindrical plastic sparger with shorten connection tube has been used, non-uniform size distribution was noticed, and it is mainly due to air losses at the connection point, which was not very well sealed (or shorten). When the cylindrical tube is attached on a straight shaped tube, similar observations like the ones made before are made. However, during the tests, larger bubbles have been noticed to be formed at the bottom of the sparger (see for example Figure 15). These large bubbles have been formed because of the larger buoyance force (depends on the bubble diameter) required for the bubble to detach the flat sparger area facing the bottom of the reactor. Considering these observations another design was used to improve the performance of the cylindrical sparger.

**Porous disks:** Clearly using porous disk as sparging device does neither produce good bubble-size distribution nor small bubbles. This is mainly because of the air loses during the aeration through the area between the disk and the sparger body resulting bubbles with irregular sizes and higher coalescing phenomena. When this area is sealed with glue, the size distribution and the bubble size have been significantly improved for the fine porous disk (the disk with porous size X has to be evaluated).

**Non-porous material:** It is commonly used in industrial applications to supply oxygen in the media as it can easily be manufactured. Through the performed testing using two tubes with 2 and 3 orifices respectively, it has been noticed that the coalescing phenomena are happening for both designs even in very low inlet air flowrates. At higher inlet air flowrates the generated bubbles are even larger and detach the surface in irregular shapes and sizes and there is always a very high possibility for bubbles coalescing.

### 4.2 Conclusions

In this project, different tests were performed to investigate the bubble generation and formation. The tests were performed using plastic and metallic spargers with porous and non-porous material under different process conditions. Through the investigation, equipment weaknesses were identified and suggestions for improved design were made. The suggestion were based on the following main observations:

Sparger material has an important role on bubble formation, small bubbles are easier to be formed when the attractive forces of the material to the bubble are small. Using the single use cylindrical

sparger and the metallic sparger one can notice that the attractive forces of the metallic sparger are higher resulting larger bubbles (See Test 1, Figure 5-Figure 10 i-ii).

Flat surfaces for plastic spargers are not particularly good unless they face upwards. When they face the bottom of the reactor (in case of porous disks or cylindrical sparger attached on straight tube) or the end surface of a cylindrical sparger attached on an L-shaped tube, the bubbles which are formed are larger either due to coalescing phenomena or increased forces required to detach the sparger. Therefore, these flat areas should always face upwards or the sparger should be re-designed without flat surfaces or minimizing the flat surfaces.

Another important observation is that the air should be forced to go through the porous material. In this way the increased bubble residence time, bubble formation with irregular shapes and sizes, and possibilities for bubbles coalescing because of bubbles generated very close are going to be avoided.

Based on the observations made through the testing, two new designs have been proposed. The designs have been partially tested, however, a final validation is to be performed when the equipment arrives.

*Note: Conclusions from validation part are to be added when it is completed.*

## 5 References

- Chisti, Y. and Moo-Young, M. (1993) 'Aeration and Mixing in Vortex Fermenters', *Journal of Chemical Technology and Biotechnology*, 58, pp. 331–336.
- Cote, P., Jean-Luc, B. and Huyard, A. (1989) 'Bubble-free aeration using membranes: mass transfer analysis', *Journal of Membr*, 47, pp. 91–106.
- Czermak, P., Weber, C., Nehring, D. and Hall, D. (2005) 'A ceramic microsparging aeration system for cell culture reactors', (1), pp. 1–6.
- Ducommun, P., Ruffieux, P., Furter, M. and Marison, I. (2000) 'A new method for on-line measurement of the volumetric oxygen uptake rate in membrane aerated animal cell cultures', 78, pp. 139–147.
- Garcia-ochoa, F. and Gomez, E. (2009) 'Bioreactor scale-up and oxygen transfer rate in microbial processes : An overview', *Biotechnology Advances*. Elsevier Inc., 27(2), pp. 153–176. doi: 10.1016/j.biotechadv.2008.10.006.
- Kazakis, N. A., Mouza, A. A. and Paras, S. V (2007) 'Experimental study of bubble formation at porous spargers', in *6th International Conference on Multiphase flow*.
- Kazakis, N. A., Mouza, A. A. and Paras, S. V (2008) 'Experimental study of bubble formation at metal porous spargers : Effect of liquid properties and sparger characteristics on the initial bubble size distribution', *Chemical Engineering Journal*, 137, pp. 265–281. doi: 10.1016/j.cej.2007.04.040.
- Martín, M., Montes, F. J. and Galán, M. A. (2008) 'Bubbling process in stirred tank reactors I : Agitator effect on bubble size , formation and rising', 63, pp. 3212–3222. doi: 10.1016/j.ces.2008.03.028.
- Schmidt, S. R. (2017) 'The Benefits and Limits of Disposable Technologies In Manufacturing Protein Therapeutic', *American Pharmaceutical Review*, pp. 1–4.
- Terasaka, K., Hirabayashi, A., Nishino, T., Fujioka, S. and Kobayashi, D. (2011) 'Development of microbubble aerator for waste water treatment using aerobic activated sludge', *Chemical Engineering Science*. Elsevier, 66(14), pp. 3172–3179. doi: 10.1016/j.ces.2011.02.043.
- Zimmerman, W. B., Tesa, V., Butler, S. and Bandulasena, H. C. H. (2008) 'Microbubble Generation', *Recent patents of Engineering*, 1, pp. 1–8.

## 6 Remaining documentation

### A.1. Pictures:

The remaining pictures are located in the google drive under the folder “Google Drive\Emmanouil\Trials”.

### A.2. Data

Table 2. Calibration data for the air-flow meter used for the trials.

Location (mm)	air flow (ccm)						
2	10.704	42	41.024	82	99.744	122	197.609
4	11.773	44	43.153	84	103.703	124	203.266
6	12.879	46	45.355	86	107.789	126	208.950
8	14.025	48	47.631	88	111.942	128	214.646
10	15.212	50	49.984	90	116.222	130	220.345
12	16.442	52	52.416	92	120.610	132	226.037
14	17.714	54	54.929	94	125.104	134	231.715
16	19.032	56	57.524	96	129.703	136	237.358
18	20.397	58	60.205	98	134.405	138	242.963
20	21.809	60	62.974	100	139.209	140	248.963
22	23.272	62	65.832	102	144.111	142	254.012
24	24.786	64	68.832	104	149.109	144	259.434
26	26.353	66	71.824	106	154.200	146	264.773
28	27.975	68	74.962	108	159.378	148	270.020
30	29.654	70	78.197	110	164.639	150	275.165
32	31.392	72	81.532	112	169.976		
34	33.189	74	84.867	114	175.389		
36	35.050	76	88.505	116	180.965		
38	36.974	78	92.146	118	186.390		
40	38.965	80	95.892	120	191.983		